



HAL
open science

The role of particle softness in determining the value of Poisson's ratio for soft sphee solids

Arkadiusz Cezary Brañka, David Michael Heyes

► **To cite this version:**

Arkadiusz Cezary Brañka, David Michael Heyes. The role of particle softness in determining the value of Poisson's ratio for soft sphee solids. *Molecular Simulation*, 2005, 31 (13), pp.935-942. 10.1080/08927020500328142 . hal-00514966

HAL Id: hal-00514966

<https://hal.science/hal-00514966>

Submitted on 4 Sep 2010

HAL is a multi-disciplinary open access archive for the deposit and dissemination of scientific research documents, whether they are published or not. The documents may come from teaching and research institutions in France or abroad, or from public or private research centers.

L'archive ouverte pluridisciplinaire **HAL**, est destinée au dépôt et à la diffusion de documents scientifiques de niveau recherche, publiés ou non, émanant des établissements d'enseignement et de recherche français ou étrangers, des laboratoires publics ou privés.

The role of particle softness in determining the value of Poisson's ratio for soft sphee solids

Journal:	<i>Molecular Simulation/Journal of Experimental Nanoscience</i>
Manuscript ID:	GMOS-2005-0042
Journal:	Molecular Simulation
Date Submitted by the Author:	18-Aug-2005
Complete List of Authors:	Brañka, Arkadiusz; Institute of Molecular Physics, PAN Heyes, David; University of Surrey, Chemistry
Keywords:	inverse-power potential, elastic constants, Poisson, auxetics, molecular dynamics simulations

SCHOLARONE™
Manuscripts

1
2
3
4
5
6
7
8
9
10
11
12
13
14
15
16
17
18
19
20
21
22
23
24
25
26
27
28
29
30
31
32
33
34
35
36
37
38
39
40
41
42
43
44
45
46
47
48
49
50
51
52
53
54
55
56
57
58
59
60

The role of particle softness in determining the value of Poisson's ratio for soft sphere solids

A.C. Brańka*

*Institute of Molecular Physics, Polish Academy of Sciences,
Smoluchowskiego 17, 60-179 Poznań, Poland*

D.M. Heyes†

*Division of Chemistry,
School of Biomedical and Molecular Sciences,
University of Surrey,
Guildford GU2 7XH, United Kingdom*

Abstract

The influence of particle softness on the Poisson's ratio of model solids has been investigated. We have used the repulsive inverse power potential ($\sim r^{-n}$ for particle separations, r) between the particles, which is conveniently characterised by one adjustable parameter, $\varepsilon = 1/n$. For large ε the interaction is soft whereas in the $\varepsilon \rightarrow 0$ limit the particles approach hard spheres. The pressure and elastic constants of the solid phase have been calculated at various densities with constant temperature molecular dynamics simulation for a range of the softness parameter in the range, $n > 12$. Density-softness surfaces of these quantities were determined which revealed hitherto unrecorded trends in the behaviour of the elastic moduli and Poisson's ratio. It was found that the pressure and some elastic properties *e.g.* the C_{12} elastic constant and the bulk modulus, manifest a maximum value or 'ridge' on this surface. The height of the maximum increases with density and interaction steepness (small ε). The Poisson's ratio varies essentially linearly with softness and is relatively insensitive to density. However, at higher densities and for larger steepness a considerable lowering of the Poisson's ratio is observed. In order to identify possible mechanisms for reducing the value of Poisson's ratio, ν , the *fluctuation* and *Born-Green* contributions were analyzed. Changes in the Poisson's ratio are mainly determined by the fluctuation contribution which can cause a considerable decrease as well as increase of its value.

PACS numbers: 62.20.Dc, 02.70.Ns, 81.40.Jj, 07.05.Tp, 81.40.Wx

Keywords: inverse-power potential, elastic constants, Poisson's ratio, auxetics, molecular dynamics simulations

*Electronic address: branka@ifmpan.poznan.pl

†Electronic address: d.heyse@surrey.ac.uk

I. INTRODUCTION

Elastic properties constitute one of the most fundamental physical properties of any material. How a body behaves under applied stress or tension is an important question for technical and industrial applications as well as having scientific interest. For relatively small deformations the elastic response is characterised by a set of elastic moduli [1]. These quantities are also relevant in the study of phase stabilities as the symmetry elements of solid phases are well reflected in the number of independent elastic constants. In fact, elastic constants can be considered to be order parameters indicative of phase stability and are therefore relevant in the study of structural transformations [2]. Indeed the fundamental distinction between a solid and fluid is marked by the absence of a (zero frequency) shear modulus in the latter [3].

Knowledge of the elastic constants greatly facilitates the design and manufacture of materials with desirable physical properties. Most of the naturally occurring materials decrease their transverse dimensions under uniaxial load. This is such a commonly observed phenomenon that only relatively recently has it been realised that the inverse situation can be observed in nature and introduced in constructed materials [4], [5] [6], [7]. Materials that expand in all directions when pulled in one direction are called *auxetics* (from the Greek 'auxetos' which can be increased). Auxetic materials are not only interesting scientifically for their rare and counter-intuitive elastic behaviour but also for a number of potentially useful technological applications [8]. This has focussed attention on what microstructurally is required to give rise to auxetic behaviour.

Even though auxetic behaviour originates on a wide range of length scales in very different naturally-occurring and man-made materials, its defining characteristic, in terms of the Pois-

1 son's ratio, ν , is always the same,
2

$$3 \quad \nu = -\frac{\eta_T}{\eta_L}, \quad (1)$$

4 where η_T and η_L are the strains in orthogonal (transverse and longitudinal) directions.
5

6
7 Poisson's ratio, the Young's, shear and bulk moduli are the basic parameters defining the
8
9 elastic response of isotropic materials. An auxetic response means a negative Poisson's ratio,
10
11 which is a convenient situation as one can basically concentrate on one well defined quantity
12
13 irrespective of the complexity of the considered system or the lengthscale on which the effect
14
15 originates. In general, in many materials, physical properties depend on direction and also the
16
17 Poisson's ratio depends on the direction of the applied stretching. In anisotropic materials,
18
19 such as crystals, ν can be positive in one direction and negative in another direction.
20
21
22
23
24
25
26
27

28 Materials with negative Poisson's ratio are quite rare in nature so the impetus is for them
29
30 to be manufactured. However, despite considerable progress, the designing and preparation
31
32 of materials with $\nu < 0$ still remains a nontrivial task and a real challenge. In particular
33
34 little progress has been reported on the synthesis of auxetics that derive this behaviour at
35
36 the molecular level [10]. This situation can be attributed to a lack of sufficient fundamental
37
38 knowledge on mechanisms leading to $\nu < 0$. Most of the modelling to date has concentrated
39
40 on idealized microstructures which by cooperative motion of the members exhibit expansion
41
42 when they are stretched. The re-entrant honeycomb structure is the most well known example
43
44 that gives auxetic behaviour, and has almost become synonymous with auxeticity [11] [12].
45
46 Cellular structures composed of geometrical elements which are vital for a negative ν , such as
47
48 the re-entrant honeycomb structure, can be achieved on different length scales and constitute
49
50 today the primary source of auxeticity [13].
51
52
53
54
55
56
57
58
59
60

1 Recently, however, a new approach has been discovered for generating auxetics which does not
2 require re-entrant features but instead employs the relative rotation of rigid units [9]. These
3 rigid units appear not to be restricted to just a few geometries. In tetrahedral frameworks,
4 the auxetic effect is achieved through synchronization of the cooperative movements of the
5 tetrahedral units [9]. Thus, it is likely that the auxetic effects may also occur if a particular
6 form of translational-rotational coupling exists in the system. In contrast to several proposed
7 models which are 'structural' or mechanical in nature there are only a few thermodynamic
8 models exhibiting auxeticity (by 'thermodynamic' here we mean that the effect originates at
9 the molecular level). The example in this category is the thermodynamically stable system of
10 2D hard cyclic hexamers [14, 15].
11
12
13
14
15
16
17
18
19
20
21
22
23
24
25
26
27

28 The connection between auxeticity and the form of interaction between constituent objects or
29 particles still needs further clarification. In particular the relationship between an interaction,
30 or its different parts, and ν is still not well understood. Establishing such a connection would
31 help us understand mechanisms leading to auxetic behaviour and possibly help to explain
32 why auxetic materials are so rare in nature and not easily manufactured. In fact, the role
33 played by particle interactions in determining the elastic constants and Poisson's ratio be-
34 haviour in general, needs to be investigated in a more systematic manner as part of this exercise.
35
36
37
38
39
40
41
42
43
44
45
46

47 As a step in this direction, we investigate the influence of repulsive interaction softness on the
48 elastic properties, and in particular on Poisson's ratio. The softness of the repulsive core is an
49 important feature of any particle interaction. For any ensemble of interacting particles to be
50 thermodynamically stable a repulsive core is required in the interparticle interaction to prevent
51 the system from collapsing [16]. The nature of this core depends on the chemical architecture
52 of the particle, and can vary considerably from very soft to extremely hard. It is worth noting
53
54
55
56
57
58
59
60

1 that particles of variable softness, usually defined through an effective repulsive potential, can
 2 now be manufactured. There is, for example growing interest in soft semi-solid systems made
 3 from colloidal and microgel particles with variable softness [17, 18][19]. So in these systems as
 4 well, establishing any general correlation between elastic properties and microscopic particle
 5 softness is desirable and can be helpful in developing better ν -controlled materials.
 6
 7
 8
 9
 10
 11
 12
 13
 14
 15

16 Among the different model interparticle potentials, the inverse-power or soft-sphere potential
 17 form is particularly suitable for investigating the role of particle softness. First of all it has the
 18 simple analytic form,
 19
 20
 21

$$22 \quad \phi(r) = \epsilon \left(\frac{\sigma}{r}\right)^n, \quad (2)$$

23 where r is the separation between two particles, σ is the particle diameter, ϵ sets the energy
 24 scale and n is a parameter determining the potential steepness (the softness is $\epsilon \sim n^{-1}$).
 25
 26
 27
 28
 29

30 Thus, the single parameter, n , changed continuously can cover a wide spectrum of practically
 31 important systems from the very soft to the extremely hard, *i.e.*, from the long-ranged Coulomb
 32 interaction ($n = 1$) to the hard sphere system ($n \rightarrow \infty$). Apart from its simplicity the inverse-
 33 power potential has many features that make this potential attractive as a model system.
 34
 35
 36
 37
 38
 39

40 From its definition in (2), we see that the inverse power potential is a self-similar function,
 41 which mixes the energy and distance scales. It can be simply represented as r^{*-n} , where
 42 $r^* = r/\sigma\epsilon^{1/n}$. An exceptional feature of the inverse power system is that the configurational
 43 properties do not depend upon the density and temperature separately but upon a particular
 44 dimensionless combination of them [20]. In effect the properties computed along one isotherm
 45 are sufficient to determine the entire phase behaviour. Depending on the softness, the r^{-n}
 46 system freezes either into the fcc or bcc crystal structure, and this softness-driven transition
 47 has been extensively studied [21–23].
 48
 49
 50
 51
 52
 53
 54
 55
 56
 57
 58
 59
 60

1
2
3
4 In this work we concentrate on thermodynamic properties, elastic constants and moduli of the
5
6 fcc solid phase of the inverse power potential. We investigate the basic thermodynamic and
7
8 mechanical quantities to establish how the interaction softness, ε , influences the elastic moduli
9
10 and Poisson's ratio.
11
12

13
14
15
16 Methods for calculation of elastic constants are briefly discussed in Sec. II. Simulation results
17
18 are presented in Sec. III and concluding remarks are made in Sec. IV.
19
20
21
22
23
24
25
26
27
28
29
30
31
32
33
34
35
36
37
38
39
40
41
42
43
44
45
46
47
48
49
50
51
52
53
54
55
56
57
58
59
60

II. CALCULATION OF ELASTIC CONSTANTS

Elastic constants are macroscopic characteristics of materials which can be determined experimentally using various techniques including Brillouin scattering, ultrasonic wave propagation, and neutron scattering. From a microscopic point of view they are N-particle averages which in many cases can be obtained from molecular simulation. In the last two decades considerable progress has been made in developing reliable simulation methods for the calculation of elastic constants of many-particle systems [24],[25],[26],[27]. Both Molecular Dynamics (MD) and Monte Carlo (MC) calculations can be performed for specified thermodynamic conditions and in various statistical mechanical ensembles [28, 29]. For example, the isoenthalpic-isotension ensemble was devised essentially to determine elastic constants by simulation [30]. So the development of new simulation methods for calculating elastic properties has also had a wider impact on the development of statistical thermodynamics.

The various approaches for calculating elastic constants can be divided into those exploiting the defining stress-strain relations by deformation of the simulation cell, and those methods exploiting fluctuation formulas for different ensembles. For example, in the strain-strain fluctuation methods the elastic constants are obtained from the fluctuations in the shape of the simulation cell *i.e.*, from fluctuations of the \mathbf{h} tensor constructed from the three vectors forming the simulation cell [28, 31]. It was found, however that the strain-strain fluctuation schemes converge slowly, at least in the dynamical MD scheme used [32, 33]. The elastic constants are more efficiently determined in the ensemble in which the \mathbf{h} tensor and hence the strain are kept fixed and the stress tensor is allowed to fluctuate [24, 34].

For our purposes the most suitable approach is the method based on the fluctuation formulas

in the canonical ensemble. This approach was invented by Squire, Holt and Hoover, [35] and has been developed and exploited in many later works (e.g., see refs., [3] and [34]). It yields isothermal elastic constants and has the advantage that all of the elastic constants can be obtained from a single simulation. Another advantage of this approach is that the reference state is not involved in the calculations. Also in the expressions for elastic constants the role of the interaction potential is more transparent than in the \mathbf{h} -fluctuation methods, and allows for a resolution of the various contributions in the hamiltonian to the elastic properties. For a system of particles interacting via a pairwise potential, $\Phi(r)$ the elastic constants can be expressed as [34]:

$$C_{\alpha\beta\lambda\tau} = \frac{1}{V} \langle \sum_{i<j} \Delta r_{ij}^{\alpha} \Delta r_{ij}^{\beta} \Delta r_{ij}^{\lambda} \Delta r_{ij}^{\tau} \frac{1}{r^2} (\Phi'' - \Phi'/r) \rangle - \frac{1}{k_B T V} \langle \delta(\sum \Delta r_{ij}^{\alpha} \Delta r_{ij}^{\beta} \Phi'/r) \delta(\sum \Delta r_{ij}^{\lambda} \Delta r_{ij}^{\tau} \Phi'/r) \rangle + \frac{N k_B T}{V} (\delta_{\alpha\lambda} \delta_{\beta\tau} + \delta_{\alpha\tau} \delta_{\beta\lambda}), \quad (3)$$

where $\Delta r_{ij}^{\alpha} = r_i^{\alpha} - r_j^{\alpha}$ and Greek indices refer to cartesian components. The symbol δ indicates the deviation of the quantity from its mean i.e., $\delta X = X - \langle X \rangle$ and $\delta_{\alpha\beta}$ is the Kronecker delta (unity when $\alpha = \beta$, zero otherwise). V is the volume of the system of N particles, k_B is Boltzmann's constant and T is the temperature. The first term in (3) is referred to as the *Born-Green* term and the second is the *fluctuation* term. The last term is the kinetic contribution, which is relatively small in solids. Thus, the elastic constants $C_{\alpha\beta\lambda\tau}$ can be considered to be composed of the sum of two terms, $C_{\alpha\beta\lambda\tau}^{BG} + C_{\alpha\beta\lambda\tau}^{FL}$, where the kinetic contribution is included in the first, the *Born-Green* term.

The above formula is for an unstressed system where the components of the reference stress tensor $S_{\alpha\beta}$ are zero. This quantity can be computed according to

$$S_{\alpha\beta} = \frac{1}{V} \langle \sum_{i<j} \Delta r_{ij}^{\alpha} \Delta r_{ij}^{\beta} \Phi'/r \rangle - \frac{N k_B T}{V} \delta_{\alpha\beta}. \quad (4)$$

For a system with isotropic reference stress, i.e., $S_{\alpha\beta} = -P \delta_{\alpha\beta} \neq 0$ the appropriate expression

1 is [34]

$$2 B_{\alpha\beta\lambda\tau} = C_{\alpha\beta\lambda\tau} + P(\delta_{\alpha\beta}\delta_{\lambda\tau} - \delta_{\alpha\lambda}\delta_{\beta\tau} - \delta_{\alpha\tau}\delta_{\beta\lambda}). \quad (5)$$

3 For not too soft interactions (*i.e.*, $n > 6$) the inverse power solids form the fcc crystal structure,
 4 which has cubic symmetry. In what follows we restrict our discussion to a system with this
 5 symmetry. For a system of spherical particles in a cubic box and axes parallel to the coordinate
 6 axes, the following elastic constants, in the more condensed Voigt's notation (where the indices
 7 1, 2, 3, 4, 5, 6 are used for xx, yy, zz, xy, xz, yz , respectively) are not zero,

$$8 C_{11} = C_{22} = C_{33},$$

$$9 C_{12} = C_{13} = C_{23},$$

$$10 C_{44} = C_{55} = C_{66}. \quad (6)$$

11 Thus, in this symmetry only three elastic constants need to be considered. The $B_{\alpha\beta\lambda\tau}$ have the
 12 same symmetry as the elastic constants $C_{\alpha\beta\lambda\tau}$, so the Voigt notation can be used and

$$13 B_{11} = C_{11} - P,$$

$$14 B_{12} = C_{12} + P,$$

$$15 B_{44} = C_{44} - P. \quad (7)$$

16 The elasticity of a system with cubic symmetry can be equivalently described by three elastic
 17 moduli: the bulk modulus B , the shear modulus G and the cubic modulus G_c [3]. They are
 18 related to the elastic constants in the following way,

$$19 B = (B_{11} + 2B_{12})/3,$$

$$20 G = (B_{11} - B_{12} + 3B_{44})/5,$$

$$G_c = (B_{11} - B_{12} - 2B_{44})/2. \quad (8)$$

The Poisson's ratio for a stretch along one of the cube axes is, [36]

$$\nu = \frac{B_{12}}{B_{12} + B_{11}} = \frac{C_{12} + P}{C_{12} + C_{11}}. \quad (9)$$

Similarly as for the elastic constants, the *Born-Green* and the *fluctuation* contribution to the above moduli can be considered separately using the decomposition, $B_{\alpha\beta} = B_{\alpha\beta}^{BG} + B_{\alpha\beta}^{FL}$, where $B_{11}^{BG} = C_{11}^{BG} - P$, $B_{12}^{BG} = C_{12}^{BG} + P$, $B_{44}^{BG} = C_{44}^{BG} - P$ and $B_{11}^{FL} = C_{11}^{FL}$, $B_{12}^{FL} = C_{12}^{FL}$, $B_{44}^{FL} = C_{44}^{FL}$. Knowing $B_{\alpha\beta}^{BG}$ and $B_{\alpha\beta}^{FL}$ we also have B, G, G_c as a sum of Born-Green and fluctuation terms, e.g., $B = B^{BG} + B^{FL}$ where $B^{FL} = (B_{11}^{FL} + 2B_{12}^{FL})/3$, and $B^{BG} = (B_{11}^{BG} + 2B_{12}^{BG})/3$. Obviously the Poisson's ratio ν is *not* $\nu^{BG} + \nu^{FL}$, but it is nevertheless informative to define and inspect the quantities ν^{BG} and ν^{FL} , as we discuss in the next section.

III. SIMULATION RESULTS

As a general remark, it is most convenient to keep formulae and calculated properties in a set of reduced units (uniquely appropriate for the r^{-n} system) where we do not need to include the temperature in a formula. Temperature effects are removed by taking into account the unique scaling feature of the inverse power system. We have in these units, for length, $\tilde{\sigma} = \sigma(\beta\epsilon)^{-\frac{1}{n}}$, so $\tilde{r} = r\sigma^{-1}(\beta\epsilon)^{-\frac{1}{n}} = r/\tilde{\sigma}$. For density $\tilde{\rho} = \rho\tilde{\sigma}^3$ and packing fraction $\tilde{\zeta} = \pi\tilde{\rho}/6$. For energy in $k_B T$, we have $\tilde{u} = \beta u$ and for the potential $\tilde{\phi} = \beta\phi = \tilde{r}^{-n}$. For the force there is $\tilde{F} = F\tilde{\sigma}/k_B T$, and $\tilde{X} = X\epsilon^{-1}\sigma^3(\beta\epsilon)^{1+\frac{3}{n}} = X\tilde{\sigma}^3/k_B T$, where X stands for pressure, elastic constant or modulus. Time is in $\tilde{t} = t(k_B T/m\tilde{\sigma}^2)^{1/2} = t(T^*\epsilon/m\tilde{\sigma}^2)^{1/2}$. In what follows we omit the tilde, so keep in mind that we are dealing with temperature-scaled quantities (also for $k_B T/\epsilon = 1$ the conventional reduced units are recovered).

Molecular dynamics simulations were performed for particles interacting via the inverse power potential (2) for a range of densities in the solid phase, $\zeta \geq 0.56$ and several values of n ranging between 14 to 144. The MD simulations were carried out on $N = 256$ particle systems with periodic boundary conditions and a standard interaction cut-off of 2.5, and 2.0 for $n > 70$. The canonical Nosé-Hoover equations of motion [37] were solved using the 4-th order Runge-Kutta algorithm, with a time step, $\Delta t = 0.001$ or 0.0005 (for $n > 70$). The reduced temperature was $T = 1$. The data were calculated from averages over $0.5 - 1$ million time step runs after equilibration and the initial positions of the particles were on fcc lattice sites. The statistical convergence of the elastic moduli by the fluctuation method is quite slow compared with the usual thermodynamic averages (*e.g.*, energy and pressure). These runs are long enough to obtain elastic properties with sufficient accuracy to observe trends on the ζ, ϵ surface.

In the simulations, the symmetry relations (6) were exploited in the calculations of C_{11} , C_{12} and C_{44} . It was verified that the calculated pressure $P = (S_{xx} + S_{yy} + S_{zz})/3$ obeys the exact relation (for the inverse power interaction), $P/k_B T \rho = 1 + n \langle u \rangle / 3$, where $\langle u \rangle$ is the average potential energy per particle.

The results for the pressure, P , are shown in Fig. 1 in which P is plotted as a function of softness for nine packing fractions in the solid phase. The lowest (dashed) curve is the melting line, determined using the Gibbs-Duhem method by Agrawal and Kofke [23] [38] for a number of values of the potential softness parameter. The points at $\varepsilon = 0$ are from the equation of state formula for the hard sphere solid [39]. From Fig. 1 it can be seen that $P(\zeta, \varepsilon)$ is not a monotonically evolving surface but has an increasingly strong ε or softness dependence at higher densities. The pressure surface contains, at any packing fraction, a maximum P_{max} which grows in height with density. The maximum indicates that the surface separates into two regions, one where $(\partial P / \partial \varepsilon)_\zeta$ is positive and the other (at higher ε) where it is negative. We can characterise the two regions respectively by either a positive or negative softness ‘compressibility’, defined as $\chi = (\partial P / \partial \varepsilon)_\zeta^{-1}$. In other words to increase pressure at a given packing fraction in the left region on the figure we have to make the potential softer, and to increase pressure in the right region it needs to be harder (*i.e.*, by increasing n).

The maximum pressure curve, P_{max} , marked on the figure as a bold solid line, starts on the melting line at $n \approx 19$ or $\varepsilon \approx 0.053$). It increases significantly for smaller $\varepsilon < 0.02$ (*i.e.*, $n > 50$) and goes towards ∞ for $\varepsilon \rightarrow 0$, *i.e.* the hard sphere limit. Figure 2 shows P_{max} as a function of the ε value where it occurs. This curve is well represented by the second order polynomial, $\zeta(\varepsilon) = \zeta^0 - 4.2367\varepsilon + 12.1813\varepsilon^2$, where $\zeta^0 = 0.7405 \cong \pi\sqrt{2}/6$ is the value of the close-packed

1 packing fraction of the hard sphere fcc structure, ζ_{cp}^{HS} [39]. Thus, for any ζ , a maximum on
 2
 3 the $P(\zeta, \varepsilon)$ surface exists at some value of the softness and its magnitude tends to infinity in
 4
 5 the hard sphere limit, *i.e.*, $\zeta = \zeta_{cp}^{HS}$ at the boundary $\varepsilon \rightarrow 0$.
 6
 7
 8
 9

10
 11 In Fig. 3 the softness dependence of the elastic constants is shown. At the lower density
 12
 13 ($\zeta = 0.58$), the ε -dependence of all three quantities is relatively weak and they are almost flat
 14
 15 lines, with the relative order $C_{11} > C_{44} > C_{12} > 0$, indicating a weak ε dependence. This
 16
 17 behaviour changes significantly on increasing density to $\zeta = 0.66$, where the ε -dependence
 18
 19 become stronger and more importantly its form is different for the three elastic constants.
 20
 21 Additionally, two regions become visible, depending on ε . In the first, representing the harder
 22
 23 systems for which ε is less than 0.02, the values of C_{11} and C_{44} are relatively insensitive
 24
 25 to ε while the C_{12} increases with softness. For softer systems, with $\varepsilon > 0.02$, all three
 26
 27 quantities decrease significantly and monotonically with increasing softness. In this second
 28
 29 region the form of the softness dependence is similar for the three elastic constants and can
 30
 31 be approximated well by an exponential. The emergence of a well-defined maximum in the
 32
 33 softness dependence of the C_{12} is a new observation.
 34
 35
 36
 37
 38
 39
 40
 41

42 In Fig. 4 examples of the elastic moduli defined in equation (8) are shown. The general
 43
 44 softness-density dependence of these moduli is similar to that of the elastic constants, with
 45
 46 a weak dependence at low densities and significant differences at higher packing fractions.
 47
 48 Furthermore there are also two regions in the ε dependence at high density. In fact the
 49
 50 distinction is even more pronounced as now both B and G_c display non-monotonic character,
 51
 52 in having a maximum. Values of the bulk modulus can also be inferred from the ratio of the
 53
 54 pressure and density differences. Thus, taking into account the definition $B = \zeta(\partial P/\partial \zeta)$ and
 55
 56 the results for the pressure surface in Fig. 1, one can expect that, for a given packing fraction,
 57
 58
 59
 60

1 the maxima in B and P have similar ε values.
 2
 3
 4
 5

6 The above results suggest that there might be a non-trivial softness dependence in other elastic
 7 properties. The quantity of primary interest here, the Poisson's ratio, is shown in Fig. 5. In
 8 its softness dependence two regions can also be distinguished. For $\varepsilon > 0.02$, $\nu(\varepsilon)$ is nearly
 9 linear in ε and, apart from the lowest density on the figure, is almost independent of density.
 10
 11 Furthermore, Poisson's ratio is well represented by the static model in which the particles are
 12 fixed on the fcc lattice sites [40], $\nu_{static} = (n+6)/(3n+6)$. For less soft systems Poisson's ratio
 13 loses its linear character and becomes strongly density dependent. For each packing fraction
 14 ν goes towards its limiting, hard sphere value, ν_{HS} which decreases from about $1/3$ close to
 15 the melting density to about $1/5$ at the close packing [40]. Figure 5 also shows that the static
 16 limiting case (bold line on the figure) is a relatively good description of the Poisson's ratio, at
 17 least for some range of the ζ, ε . The static model means that the fluctuation contributions are
 18 not taken into account, and that for the Poisson's ratio formula, only the Born-Green terms
 19 are retained. This approximation gives a '*Born-Green Poisson's ratio*',
 20
 21
 22
 23
 24
 25
 26
 27
 28
 29
 30
 31
 32
 33
 34
 35
 36
 37
 38
 39

$$\nu_{BG} = B_{12}^{BG} / (B_{12}^{BG} + B_{11}^{BG}), \quad (10)$$

40 which is shown in Fig. 6 for several packing fractions. From the figure it can be seen that
 41 ν_{BG} is a fairly regular, almost linear function of ε with a slope practically equal to that of the
 42 static model line. Only for the soft systems ($\varepsilon > 0.05$) is a slight bend away from linearity
 43 observed. Also we note that the density dependence is considerably weaker than the softness
 44 dependence. A variation of ζ over the entire solid phase causes only a minor change (typically
 45 a few percent) in the ν_{BG} value for any ε . As can be seen in the figure, on increasing ζ , the
 46 nearly colinear curves approach from below the static model line. Thus, the static result can
 47
 48
 49
 50
 51
 52
 53
 54
 55
 56
 57
 58
 59
 60

be a good starting point for quantitative description of ν_{BG} , and it can be seen that significant changes in Poisson's ratio are achieved by varying ε rather than ζ in the available parameter range.

A comparison between Figs. 5 and 6 indicates that changes in $\nu(\zeta, \varepsilon)$ are mainly determined by the fluctuation terms and more importantly they can cause a considerable decrease as well as increase of the Poisson's ratio. Their role becomes more transparent after writing Poisson's ratio in a form explicitly featuring ν_{BG} ,

$$\frac{\nu}{\nu_{BG}} = \left(1 - \frac{B_{12}^{FL}}{B_{12}^{BG}}\right) \left(1 - \frac{B_{12}^{FL} + B_{11}^{FL}}{B_{12}^{BG} + B_{11}^{BG}}\right)^{-1}. \quad (11)$$

From the above definition it follows that to lower the value of the Poisson's ratio, *i.e.*, to get $\nu/\nu_{BG} < 1$, in the inverse power system, the following condition has to be obeyed,

$$\frac{B_{12}^{FL}}{B_{12}^{BG}} > \frac{B_{11}^{FL}}{B_{11}^{BG}}, \quad (12)$$

or

$$\frac{B_{12}^{FL}}{B_{11}^{FL}} > \frac{B_{12}^{BG}}{B_{11}^{BG}}. \quad (13)$$

Figure 7 shows a plot of the two ratios in equation (13) against ε , to explore the above criterion. The division of two fluctuation quantities unfortunately leads to some scatter in the data points. Nevertheless certain trends can be identified, and these are represented by the fitted lines (second order polynomials) shown on the figure. It is evident from this figure that it is the *fluctuation* ratio B_{12}^{FL}/B_{11}^{FL} which changes most with packing fraction and the softness parameter. This ratio predominately decreases with increasing ε and its magnitude is comparable to the *Born-Green* ratio for intermediate values of the

1 softness. The generally opposite softness dependence of these ratios means that all possi-
2 bilities, of B_{12}^{FL}/B_{11}^{FL} being less than, equal to, and greater than B_{12}^{BG}/B_{11}^{BG} occur on the
3 figure. Hence, respectively $\nu > \nu_{BG}$, $\nu = \nu_{BG}$ and $\nu < \nu_{BG}$, can be satisfied at any given density.
4
5
6
7
8
9

10 From Fig. 7 it can be seen that at lower densities, the fluctuation ratio bends toward the
11 Born-Green ratio for $\varepsilon \rightarrow 0$ (see the data for $\zeta = 0.58$). This indicates that for some range of
12 the softness and packing fractions close to the melting the Poisson's ratio is *lower* than that of
13 the hard spheres. That $\nu < \nu_{HS}$ (and the possible presence of a small minimum in Fig. 5 for
14 $\zeta = 0.58$) is an unexpected result. The lowest value of ν for the lower packing fractions close
15 to the melting value is therefore not the hard sphere value.
16
17
18
19
20
21
22
23
24
25
26
27
28
29
30
31
32
33
34
35
36
37
38
39
40
41
42
43
44
45
46
47
48
49
50
51
52
53
54
55
56
57
58
59
60

IV. CONCLUSIONS

In this work the influence of interparticle interaction softness on the solid phase elastic properties has been investigated, particularly for Poisson's ratio, ν . The canonical ensemble MD simulation method of Nosé and Hoover was used and the stress fluctuation scheme was applied to obtain the isothermal elastic constants of the fcc phase. The elastic constants and elastic moduli were determined for a range of the softness parameter ($\varepsilon \equiv 1/n$) of the soft-sphere potential and covering most of the solid phase. This data was used to construct density-softness surfaces of these properties. The determination of the elastic constants from the simulations is time consuming and so the results to date only indicate trends. More quantitative conclusions will have to wait for more extensive simulations to be carried out. One characteristic feature which emerges from these studies is the existence of a maximum in the pressure and the elastic constant C_{12} on a plot of these quantities against the particle softness (ε) for constant density (ζ) systems. Locating the elastic constant maxima in terms of the value of softness for each density (as we have done for the pressure) requires more extensive simulations.

Two other moduli, B and G_c defined in Section 2 also exhibit maxima. In all cases the height of the maximum increases with increasing density. In the case of the pressure the maximum line starts at the melting density for $n \approx 19$ and terminates at close packing of the hard sphere fcc structure ($\zeta = 0.7405$). For all calculated elastic properties it is possible to distinguish two regions in their density-softness dependence. One, roughly for $\varepsilon > 0.02$ where a weak ζ -dependence and fairly regular ε -dependence is present. In this region the Poisson's ratio is predominately linear and hardly modified by density. In the second region of larger interaction steepness (smaller ε), considerable variation in ν with density and softness is evident. From the point of view of the auxetic behaviour this may be an interesting

1 region as considerable lowering of the value of the Poisson's ratio can be achieved by slight
2 modification of the interaction softness, particularly at higher packing fraction. Therefore for
3 steep interaction particle systems, small variations in the density and softness can have a sig-
4 nificant affect on the Poisson's ratio. This possibility seems not to have been fully exploited yet.
5
6
7
8
9

10 It was demonstrated that the *Born-Green* Poisson's ratio, ν_{BG} , is well represented by the static
11 case and is almost density independent, suggesting that the fluctuation part plays an important
12 role in determining Poisson's ratio. It was found that it is the ratio of the fluctuation part of
13 the elastic constants, B_{12}^{FL}/B_{11}^{FL} that is responsible for significant changes both in magnitude
14 and form of $\nu(\zeta, \varepsilon)$. We have found that for the inverse power potential fcc solid, $\nu > \nu_{BG}$
15 for such ζ, ε for which the ratio $B_{12}^{FL}/B_{11}^{FL} < B_{12}^{BG}/B_{11}^{BG}$. Therefore an important, potentially
16 useful outcome of this work is the observation that the fluctuation part can not only diminish
17 ν but also may causes an increase of its value.
18
19
20
21
22
23
24
25
26
27
28
29
30
31
32
33
34

35 To obtain the desired effect, (*i.e.*, a decrease of Poisson's ratio value) augmentation of the
36 fluctuation part should take place in an appropriate range of softness and state parameters. It
37 is not sufficient to *just* make the system harder (*i.e.*, decrease ε) to get a noticeable lowering
38 of Poisson's ratio (see the data for $\zeta = 0.58$ in Fig. 5), but it is also necessary to increase the
39 packing fraction. For the inverse power solid the appropriate range can be considered to be in
40 the region *ca.* $n > 50$ and $\zeta \geq 0.66$ (it worth to add that in this region the relative contributions
41 of the fluctuation part to the Poisson's ratio becomes greater than that of the Born-Green part
42 or $\nu_{FL}/\nu_{BG} > 1$). It is perhaps not surprising that the fluctuation term is so important in
43 potentially lowering Poisson's ratio, as it is the cooperative motion of the building components
44 that has been found responsible for giving auxeticity in most the known examples.
45
46
47
48
49
50
51
52
53
54
55
56
57
58
59
60

Acknowledgements

The authors thank The Royal Society (London) and the Polish Academy of Sciences for partly funding this collaboration. We are grateful to K.V. Tretiakov and K.W. Wojciechowski for providing computer simulation data for the hard sphere Poisson's ratio prior to publication. The work has been partially supported by the Polish Committee for Scientific Research (KBN) grant No. 4T11F01023.

For Peer Review Only

References

-
- [1] J.H. Wallace, *Statistical Mechanics of Elasticity* (Wiley, New York, 1972).
- [2] L.D. Landau, E.M. Lifshic, A.M. Kosevich, and I.P Pitaevskii, *Theory of Elasticity* (Pergamon Press, London,1986).
- [3] S. Hess. M. Kröger and W.G. Hoover. Shear modulus of fluids and solids. *Physica A*, **239**, 449 (1997).
- [4] R. Lakes. Foam Structures with a Negative Poisson's Ratio. *Science*, **235**, 1038 (1987).
- [5] B.D. Caddock and K. Evans. Microporous materials with negative Poisson's ratios. I. Microstructure and mechanical properties. *J. Phys. D*, **22**, 1877 (1987).
- [6] R.H. Baughman, J.M. Shacklette, A.A. Zakhidov, and S. Stafström. Negative Poisson's ratios as common feature of cubic materials. *Nature*, **392**, 362 (1998).
- [7] K.L. Alderson, V.R. Simkins, V.L. Coenen, P.J. Davies, A. Alderson and K.E. Evans. How to make auxetic fibre reinforced composites. *phys. stat. sol.(b)*, **242**, 509 (2005).
- [8] K.E. Evans and A. Alderson. Auxetic Materials: Functional Materials and Structures from Lateral Thinking!. *Adv. Mater.*, **12**, 617 (2000).
- [9] A. Alderson and K.E. Evans, Molecular Origin of Auxetic Behavior in Tetrahedral Framework Silicates, *Phys. Rev. Lett.* **89**, 225503 (2002).
- [10] C. He, P. Liu, P.J. McMullan and A.C. Griffin. Toward molecular auxetics: Main chain liquid crystalline polymers consisting of laterally attached para-quaterphenyls. *phys. stat. sol.(b)*, **242**, 576 (2005).
- [11] K.E. Evans, M.A. Nkansah, I.J. Hutchinson, and S.C.Rogers. Molecular network design. *Nature*, **353**, 124 (1991).

- 1
2
3
4
5
6
7
8
9
10
11
12
13
14
15
16
17
18
19
20
21
22
23
24
25
26
27
28
29
30
31
32
33
34
35
36
37
38
39
40
41
42
43
44
45
46
47
48
49
50
51
52
53
54
55
56
57
58
59
60
- [12] A. Alderson, J. Rasburn, S. Ameer-Beg, P.G. Mullarkey, W. Perrie, and K.E. Evans. An auxetic filter: A tuneable filter displaying enhanced size selectivity or defouling properties. *Ind. Eng. Chem. Res.*, **39**, 654 (2000).
- [13] A. Spadoni, M. Ruzzene and F. Scarpa. Global and local linear buckling behavior of a chiral cellular structure. *phys. stst. sol. (b)*, **242**, 695 (2005).
- [14] K.W. Wojciechowski. Constant thermodynamic tension Monte Carlo studies of elastic properties of a two-dimensional system of hard cyclic hexamers. *Mol. Phys.*, **61**, 1247 (1987).
- [15] K.W. Wojciechowski and A.C. Brańka. Negative Poisson's ratio in a two-dimensional "isotropic" solid. *Phys. Rev. A*, **40**, 7222 (1989).
- [16] D. Ruelle, *Statistical Mechanics Rigorous Results*, (W.A. Benjamin, INC, 1969).
- [17] J.G. Zhang, S.Q. Xu SQ and E. Kumacheva. Polymer microgels: Reactors for semiconductor, metal, and magnetic nanoparticles. *J. Amer. Chem. Soc.*, **126**, 7908 (2004).
- [18] B.H. Tam, K.C. Tam, Y.C. Lam and C.B. Tan. A Semi-Empirical Approach for Modeling Charged Soft Microgel Particles. *J. Rheol.*, **48**, 915 (2004).
- [19] J. Mewis, W.J. Frith, T.A. Strivens and W.B. Russel. The rheology of suspensions containing polymerically stabilized particles. *AIChE Journal*, **35**, 415 (1989).
- [20] W.G. Hoover, S.G. Gray and K.W. Johnson. Thermodynamic Properties of the Fluid and Solid Phases for Inverse Power Potentials. *J. Chem. Phys.*, **55**, 1128 (1971).
- [21] W.G. Hoover, D.A. Young and R. Grover. Statistical Mechanics of Phase Diagrams. I. Inverse Power Potentials and the Close-Packed to Body-Centered Cubic Transition. *J. Chem. Phys.*, **56**, 2207 (1972).
- [22] B.B. Laird and A.D.J. Haymet. Phase diagram for the inverse sixth power potential system from molecular dynamics computer simulation. *Molec. Phys.*, **75**, 71 (1992).
- [23] R. Agrawal and A.D. Kofke. Solid-Fluid Coexistence for Inverse-Power Potentials. *Phys. Rev.*

- 1 Lett., **74**, 122 (1995).
- 2
- 3
- 4 [24] J.R. Ray, M.C. Moody, and A. Rahman. Calculation of elastic constants using isothermal molec-
- 5 ular dynamics. Phys. Rev. B, **33**, 895 (1986).
- 6
- 7
- 8
- 9 [25] A.A. Gusev, M.M. Zehnder, and U.W. Suler. Fluctuation formula for elastic constants. Phys.
- 10 Rev. B, **54**, 1 (1996).
- 11
- 12
- 13
- 14 [26] K.W. Wojciechowski, K.V. Tretiakov, A.C. Brańka, and M. Kowalik. Elastic properties of two-
- 15 dimensional hard disks in the close-packing limit. J. Chem. Phys., **119**, 939 (2003).
- 16
- 17
- 18
- 19 [27] K. Van Workum and J.J. Pablo. Improved simulation method for the calculation of the elastic
- 20 constants of crystalline and amorphous systems using strain fluctuations. Phys. Rev.E, **67**, 011505
- 21 (2003).
- 22
- 23
- 24
- 25
- 26 [28] J.R. Ray and A. Rahman. Statistical ensembles and molecular dynamics studies of anisotropic
- 27 solids. II. J. Chem. Phys. **82**, 4243, (1985).
- 28
- 29
- 30
- 31 [29] Z. Zhou. Fluctuations and thermodynamis properties of the constant shear strain ensemble. J.
- 32 Chem. Phys., **114**, 8769 (2001).
- 33
- 34
- 35
- 36 [30] J.R. Ray and A. Rahman. Statistical ensembles and molecular dynamics studies of anisotropic
- 37 solids. J. Chem. Phys., **80**, 4423 (1984).
- 38
- 39
- 40
- 41 [31] M. Parrinello and A. Rahman. Polymorphic transitions in single crystals: A new molecular dy-
- 42 namics method. J. Appl. Phys., **52**, 7182 (1981).
- 43
- 44
- 45
- 46 [32] M. Sprik, R.W. Impey, and M.L. Klein. Second-order elastic constants for the Lennard-Jones
- 47 solid. Phys. Rev. B, **29**, 4368 (1984).
- 48
- 49
- 50
- 51 [33] J. Ray. Elastic constants and statistical ensembles in molecular dynamics. Comp. Phys. Rep., **8**,
- 52 109 (1988).
- 53
- 54
- 55
- 56 [34] Z. Zhou and B. Joós. Stability criteria for homogeneously stressed materials and the calculation
- 57 of elastic constants. Phys. Rev. B, **54**, 3841 (1996).
- 58
- 59
- 60

- 1
2 [35] D.R. Squire, A.C. Holt, and W.G. Hoover. Isothermal elastic constants for argon. Theory and
3
4 Monte Carlo calculations. *Physica*, **42**, 388 (1969).
5
6
7 [36] S.P. Tokmakova. Stereographic projections of Poisson's ratio in auxetic crystals. *phys. stst. sol.*
8
9 (b), **242**, 721 (2005).
10
11 [37] W.G. Hoover. Canonical dynamics: Equilibrium phase-space distributions. *Phys. Rev. A*, **31**,
12
13 1695 (1985).
14
15
16 [38] R. Agrawal, and A.D. Kofke. Phase diagram for the inverse sixth power potential system from
17
18 molecular dynamics computer simulation. *Molec. Phys.*, **85**, 23 (1995).
19
20
21 [39] K.R. Hall. Another hard sphere equation of state. *J. Chem. Phys.*, **57**, 2252 (1971).
22
23
24 [40] K.V. Tretiakov and K.W. Wojciechowski. Poisson's ratio of the fcc hard spheres at high densities.
25
26 to appear in *J. Chem. Phys.* (2005).
27
28
29
30
31
32
33
34
35
36
37
38
39
40
41
42
43
44
45
46
47
48
49
50
51
52
53
54
55
56
57
58
59
60

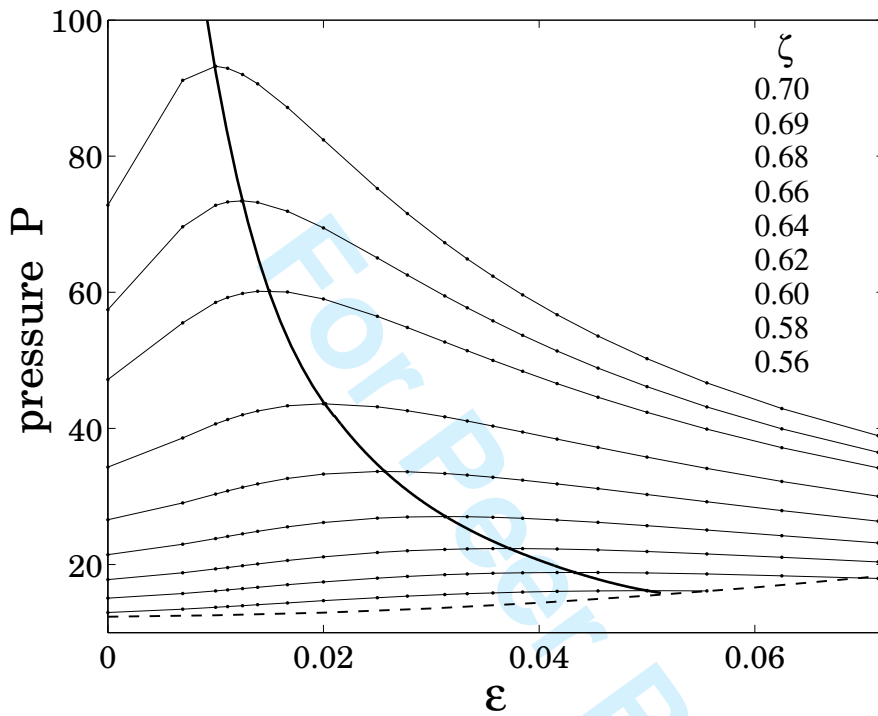


FIG. 1: The pressure, $P(\zeta, \varepsilon)$ - surface, of the inverse-power solid. The lowest line is the melting curve determined by Agrawal and Kofke [38]. The edge ($\varepsilon = 0$) points are taken from the hard sphere equation of state by Hall [39]. The bold line is the demarcation or maximum pressure line.

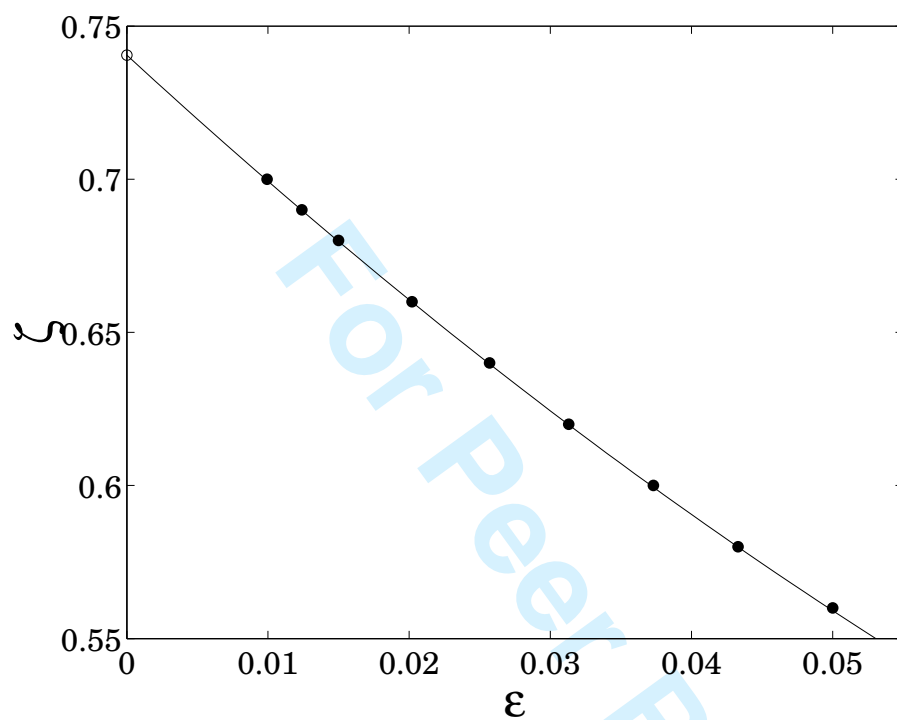


FIG. 2: The softness and packing fractions for which the maximum pressure line in Fig. 1 is the locus.

The points are from maximum condition $(\partial P/\partial \epsilon)_\zeta = 0$ and are well represented by the polynomial:

$\zeta^0 - 4.2367\epsilon + 12.1813\epsilon^2$, drawn in the figure as the solid line. ζ^0 , marked as the open circle, is the

close packed density of the fcc hard sphere structure.

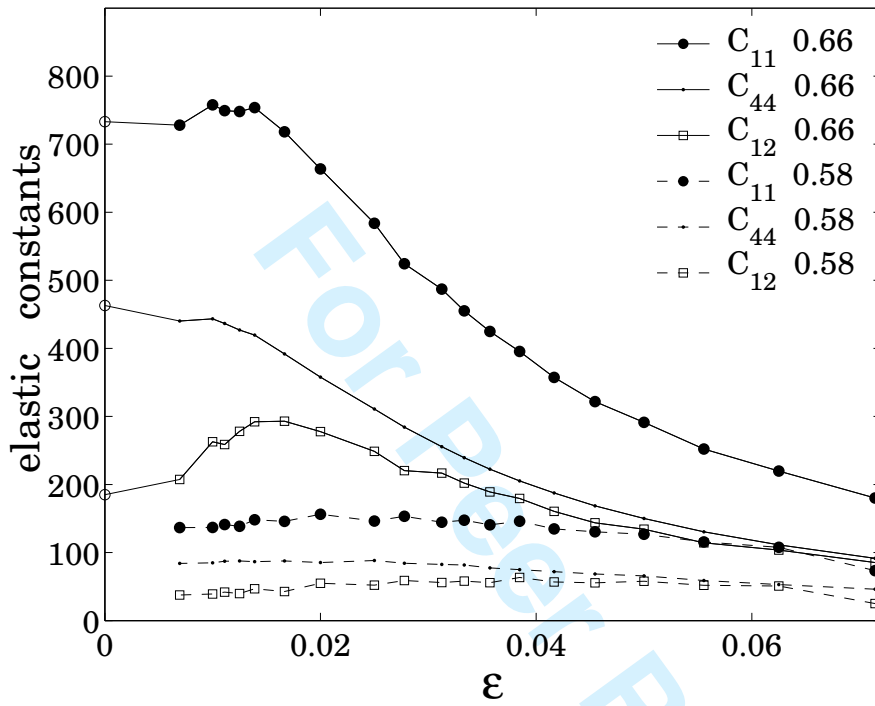


FIG. 3: The elastic constants defined in equations (3) and (6) against the interaction softness ϵ for the fcc solid of the inverse power system, and for two packing fractions (indicated on the figure).

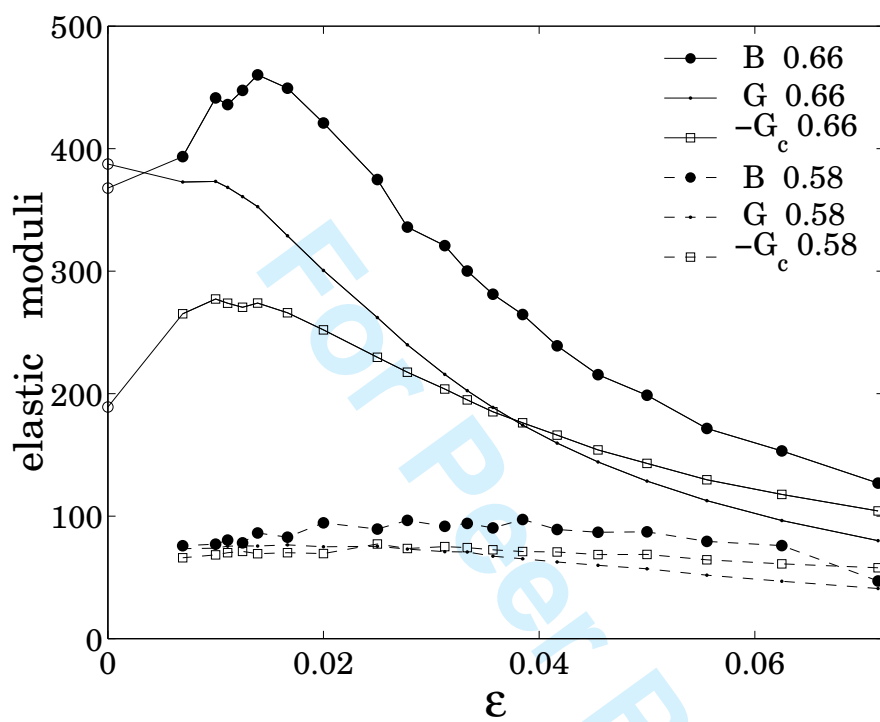


FIG. 4: The bulk, shear and cubic moduli defined in equation (8) of the inverse power solid against the interaction softness for the same conditions as in Fig. 3.

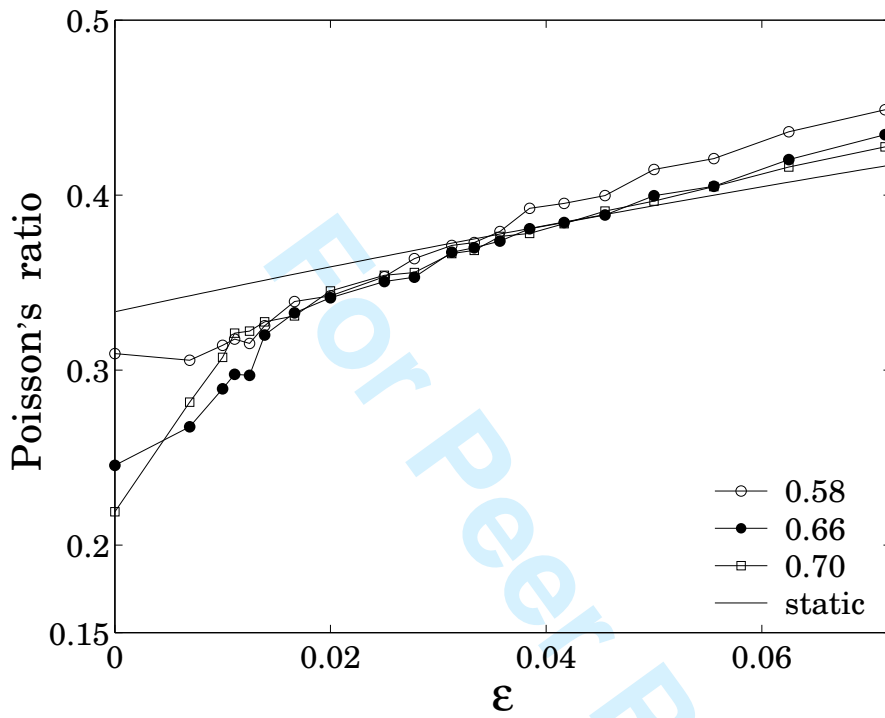


FIG. 5: The Poisson's ratio, ν , of the fcc solid of the inverse power system against the interaction softness ϵ for different packing fractions (symbols). The bold line represents the static case and the edge ($\epsilon = 0$) points are the Poisson's ratio of the fcc hard sphere solid by Tretiakov and Wojciechowski [40].

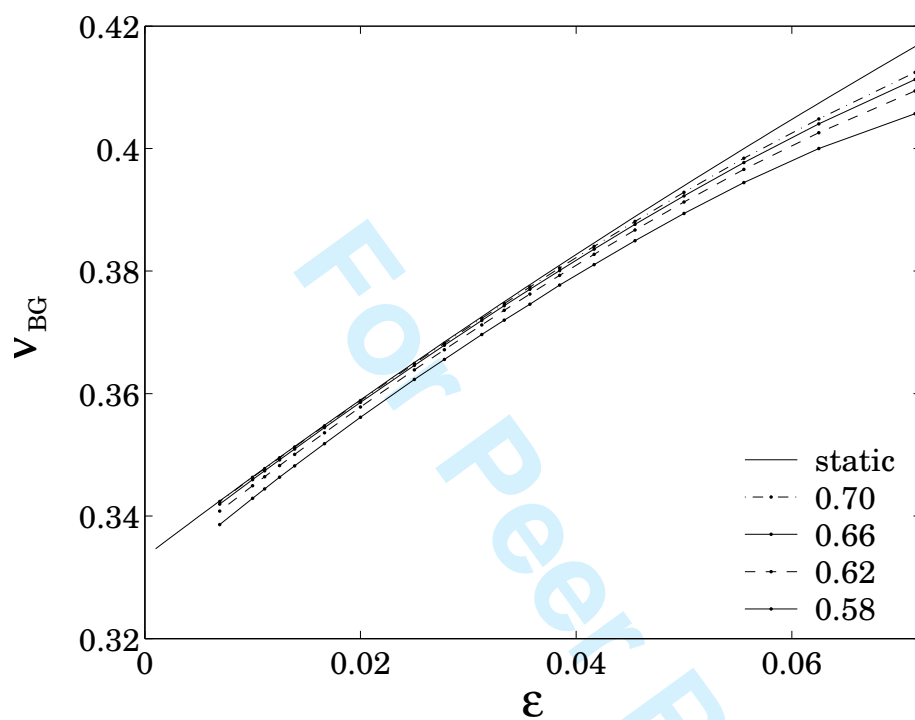


FIG. 6: The *Born-Green* Poisson's ratio, ν_{BG} (*i.e.*, ν with no fluctuation contributions) as a function of the particle softness. The lines for different packing fractions go toward the static case line in the limit of close packing.

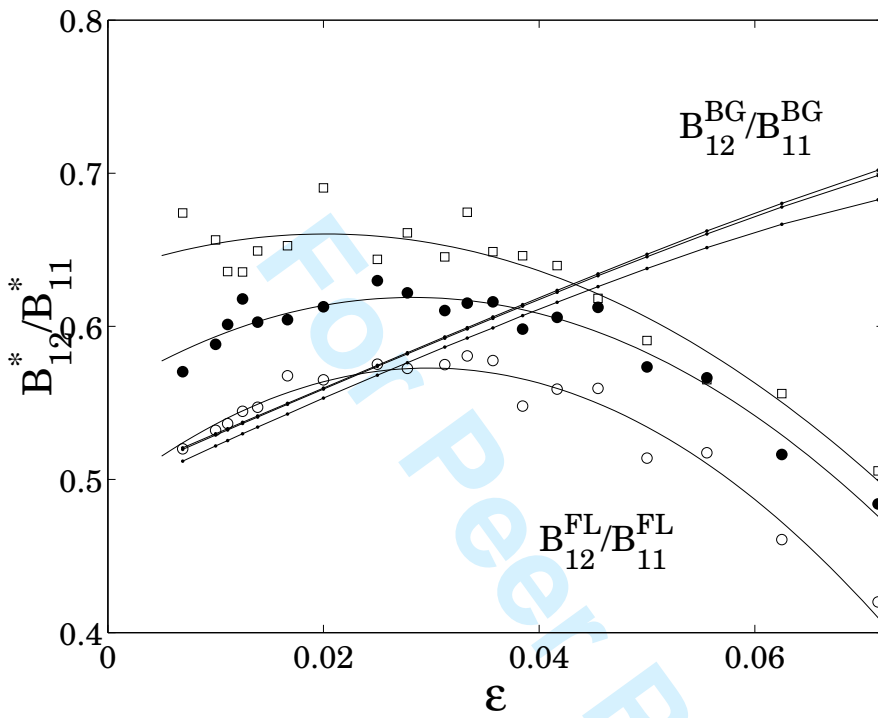


FIG. 7: The ratio of the *Born-Green* parts and *fluctuation* parts (symbols) of elastic constants for the three packing fraction used in Fig. 5. The symbols used for the different packing fractions are the same in the two figures